Micromechanical Analysis of Polymer-Nanofiber Composites

C. Rebecca Locker[1,*], Jorgen Bergstrom[2], Xiaohu Liu[2], Andy H. Tsou[1], Viktor B. Buchholz[1], and Aspy K. Mehta[3]

[1]ExxonMobil Research and Engineering Company, Corporate Strategic Research, 1545 Rt. 22E, Annandale, NJ 08801, [*]c.rebecca.locker@exxonmobil.com
[2]Veryst Engineering LLC, 47A Kearney Rd., Needham, MA 02494
[3]ExxonMobil Chemical Company, Chemical Research, 4500 Bayway Drive, Baytown, TX 77520

ABSTRACT

A micromechanical model is developed for composite materials with distinct material domains that differ in length scales. Representative volume elements (RVEs) of a nanofiber-filled polymer are generated for finite element simulations using Abaqus™ software. A stochastic method is developed to create 3D RVEs that statistically represent the high aspect ratio nanofiber composites. Thermo-mechanical properties for a particular system are computed and found to be comparable to the Cox-Krenchel model and to experiments. The model is extended to include a rubber domain that is 20 times greater than the nanofiber diameter. The results are compared to the binary system using linear material models. Advanced material models are then used to establish relationships between fiber dispersion microstructure (fiber dimension, orientation, and degree of loading) and resulting thermo-mechanical properties (modulus and thermal expansion coefficient) in the ternary system.

Keywords: micromechanical, finite element method, polymer nanocomposite, stochastic representative volume element, nonlinear materials

1 INTRODUCTION

Nanofibers have emerged as promising polymer additives because of their potential to enhance thermo-mechanical properties of the polymer more efficiently than conventional filler materials such as glass fiber and talc. While these compounds have the potential to be the next generation light-weight structural plastic materials, many critical physical properties like modulus, toughness, heat distortion temperature and thermal expansion coefficient, are quite sensitive to the filler compositions and processing (mixing) conditions. Contolling the processing conditions remains an industrial challenge, but there is strong potential to design materials based on the microstructure of the fillers (including chemical structure and shape, as well as degree of dispersion within the continuous phase) that will exhibit desired physical properties. The fundamental relationship between the composite microstructure (orientation, dispersion, and dimensions of the filler phase) and the thermal and mechanical properties must be understood in order to implement a rational material design strategy.

In this work, micromechanical models of polymer-nanofiber and polymer-rubber-nanofiber systems have been developed to compute the modulus, coefficient of linear thermal expansion (CLTE) and heat distortion temperature using a commercial non-linear finite element code. These micromechanical models were used to establish a quantitative structure-property relationship between the fiber microstructure (fiber dimension, orientation, degree of loading) and the resulting composite properties and to guide material design for structural applications.

2 MICROMECHANICAL MODEL

High aspect ratio nanofibers present a computational challenge for finite element simulations because the mesh size must be smaller than the smallest length scale of interest. To overcome this computational burden, representative volume elements are generated stochastically with periodic boundaries as discussed in detail below.

2.1 Stochastic representative volumes

In order for the model "unit cell" to be statistically representative of a real polymer-nanofiber composite, a stochastic method is developed to generate 3D RVEs. Linear fibers are placed inside the RVE according to a prescribed statistical distribution (random, uniform or Gaussian) without overlap, allowing for fiber loadings that exceed the theoretical upper limit derived from a 2D random planar fiber orientation. Due to the fibers' high aspect ratio (AR), the resulting RVEs are non-cubic with periodic boundary conditions. The minimum required RVE dimensions were determined iteratively based on convergence of the computed tensile modulus values. Fig. 1 shows examples of RVEs developed for the polymer/nanofiber binary system with varying fiber oreintations and loadings.

2.2 Material models

For the binary polymer/nanofiber systems, all materials are assumed to follow a linear constitutive equation ($\sigma=E\varepsilon$) where the stress, σ, is proportional to the strain, ε, and the

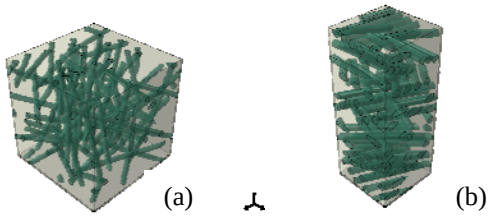

Figure 1: Optimized 3D representative volumes for the binary polymer (grey) /nanofiber (green) composite.(a) 3D random fiber orientation with fiber angles chosen from a spherical distribution. (b) 2D random in-plane fiber orientation with fiber angles chosen from a gaussian distribution with a mean of 0°(planar) and variance of +/- 5°.

Young's modulus, E, is the proportionality constant. Experimentally measured tensile modulus and Poisson's ratio ($\nu=-d\varepsilon_{trans}/d\varepsilon_{axial}$) of the pure components are used as inputs for the tensile modulus simulations of the composite materials.

The ternary polymer/nanofiber/rubber simulations have the option of using either all-elastic material models described above or advanced nonlinear material models for the polymer and rubber components. The advanced material model for the polymer treats the polymer as a viscoelastic material and experimentally measured stress relaxation curves are fit to the 3-network model [1]. The material model is calibrated with the PolyUMod library developed by Veryst Engineering LLC that runs under Abaqus™ finite element software. The 3-network model has been shown to reproduce measured stress-strain curves in cyclic loading experiments for polymers of interest.

The rubber phase of the micromechanical model can be treated as a nonlinear viscoplastic material using the Bergstrom-Boyce model [2]. The Bergstrom-Boyce model accurately predicts stress-strain behavior of elastomeric materials even at high strains ($\varepsilon>6$).

2.3 Finite Element Analysis

To compute the tensile modulus of each RVE, E_i, the RVE is subjected to a uniaxial strain of $\varepsilon/\varepsilon_0=0.001$in axial and transverse directions using the Abaqus™ finite element software. The tensile modulus is computed as the ratio of stress to strain. The coefficient of linear thermal expansion (CLTE, $\alpha=(1/\ell)d\ell/dT$) is computed for each RVE in the axial ($\alpha_{a,i}$) and transverse ($\alpha_{t,i}$) directions after being subjected to a temperature increase from 273K to 283K. In this case, the experimentally measured CLTE of the polymer is used as an input, and the CLTE of the fibers is assumed to be zero.

A total of N RVEs with identical dimensions and statistical fiber distributions but with different fiber microstructures are considered to be in the same RVE class. The computed thermo-mechanical responses of these composites are statistically averaged over responses from all the RVEs within one class so an average material response can be computed as $A=\sum_{i=1,N} A_i / N$. This approach computes average properties without suffering from convergence issues associated with finite element deformation simulations of larger RVEs. The minimum number of RVEs, N, required to achieve reasonable standard errors in the mean values of the averaged moduli and CLTE differs for each RVE class, but is around N=100 for all cases presented here.

3 COX-KRENCHEL MODEL

For linear materials, a simple rule-of-mixtures semi-empirical model may be used to predict the compound modulus and thermal expansion. The Cox-Krenchel (CK) model [3,4] for discontinuous fiber-filled materials has been shown to give reasonable approximations for nanofiber-filled polymer systems [5] and is given by:

$$E_c = \eta_l \eta_\theta E_f v_f + E_m (1 - v_f), \quad (1)$$

where E is the modulus, v is the volume fraction and the subscripts c, f, and m correspond to the composite, fiber and matrix, respectively. The fiber correction factors account for the finite length of the fibers (η_l) and the average fiber orientation (η_θ) as described in Ref. 3.

The CLTE has been derived in Ref. [6] for an isotropic continuous fiber and matrix composite system. The Cox-Krenchel approach has been used to generalize the CLTE to account for discontinuous fibers [7] and the fiber orientation [8] to give:

$$\alpha_{xy} = (\eta_l \eta_\theta E_f \mathrm{v}_f \alpha_f + E_m \mathrm{v}_m \alpha_m)/\mathrm{E}_c , \quad (2)$$

for expansion in the axial directions, and

$$\alpha_z = (1 - v_f)\mathrm{v}_f \alpha_f + (1 - v_m)\mathrm{v}_m \alpha_m , - v_c \alpha_{xy} \quad (3)$$

for expansion in the transverse direction where xy is the axial plane, z is the transverse direction, ν is Poisson's ratio and α is the linear expansion coefficient. All pure component properties in the CK equations are computed from experimental measurements. For the results presented here, the fibers are assumed to be in a 2D planar orientation to give $\eta_\theta=3/8$ and η_l is computed from the fiber dimensions supplied by the vendor.

4 RESULTS

Tensile modulus and thermal expansion coefficients are computed as a function of nanofiber concentration and compared to experimental results measured from nanofiber (NF1, AR=40) reinforced polymer nanocomposites. The results are compared to the CK equations for non-

continuous fiber-reinforced systems to validate the simulation protocol. Systematic studies with a different nanofiber (NF2, AR=700) are presented to evaluate the impact of the materials choice on composite properties. Rubber domains are added to NF1-polymer nanocomposites to screen for desired material properties in the ternary system.

4.1 Polymer-nanofiber system

Composite modulus and CLTE of the binary system are computed using the finite element method described above assuming linear material properties and perfect bonding between the polymer matrix and the nanofibers. Fig. 2 compares the results to those obtained from the Cox-Krenchel model and experimentally measured values for the Polymer/NF1 system. Fig. 2a compares the modulus as a function of nanofiber loading. The RVE snapshots in Fig. 2c show the Mises stresses in the fibers after deformation in the axial (left) and transverse (middle) directions. The snapshots clearly show that stress is transferred from the polymer to the stiffer nanofiber effectively when fibers are aligned in the strain direction, but there is essentially no stress transferred in the fiber's radial direction during transferse deformation. This is consistent with the computed composite moduli: for 2D planar systems, the modulus is higher in the axial direction than in the transverse direction for all fiber loadings. The Cox-Krenchel model's overprediction of the composite modulus increases with fiber loading. This is likely due to non-ideality of the experimental system including the assumptions of 2D planar fiber orientation and perfect fiber dispersion. The FEA simulation results are lower than what is predicted by the Cox-Krenchel model and they accurately predict the composite modulus within experimental error. In the FEA simulation the fibers within the RVE are not perfectly planar: there is a Gaussian distribution of fiber orientations with a planar mean, but a variance of 5 degrees. This fiber orientation is more realistic and thus agrees better with experiment. However, the moduii computed from the FEM simulations are systematically higher than experiment. This can be attributed to fiber aggregation in the real system that disallows full transfer of stress from the matrix to the individual fibers. In some systems, high AR nanofibers have been observed to curve within the matrix, further decreasing the load transfer under axial strain. This was not observed experimentally for the NF1 compounds.

Eqns. 2 and 3 are used to compute CLTE for a 2D planar NF1/polymer system and the results are shown in Fig. 2b. The results are consistent with those of the computed modulus in Fig. 2a. The Cox-Krenchel model systematically underpredicts the experimenally measured CLTE for all fiber loadings, and the FEM results are comparable to the experimental results at low loadings. Deviations are attributed to the assumptions of 2D planar fiber orientation in the CK model and perfect dispersion in the model and the simulations. A snapshot of the distribution of Mises stresses after thermal loading is shown in Fig. 2d.

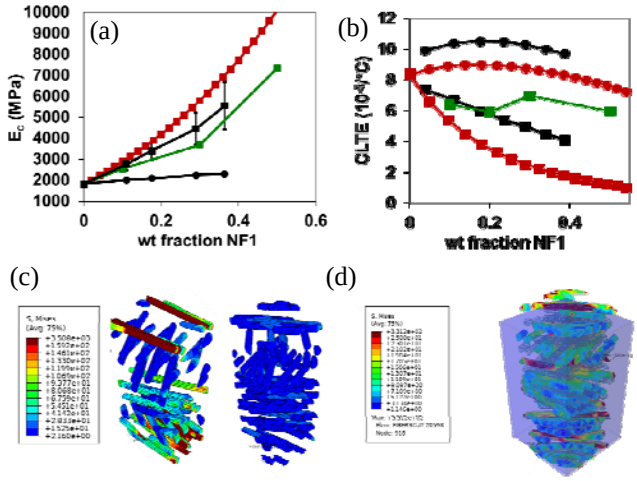

Figure 2**:** (a) Composite modulus of NF1/polymer system in the axial direction (squares, along fiber axis) computed from the CK model (red squares, for random 2D fiber orientation), experimentally measured (green squares, from flexural modulus test), and from FEM simulations (black squares). The modulus in the transverse direction computed from FEM (black circles, transverse to fiber axis) is also shown. (b) Coefficient of linear thermal expansion (CLTE) of NF1/polymer system. FEM results at T=279K (black squares) underestimate expansion in the machine direction when compared to experimental values at T=240K (green squares). Expansion in the normal direction is predicted by FEM to be greater than in the machine direction (black circles). (c) The distribution of Mises stresses in the fibers in one representative RVE at 40 wt% fiber loading is shown below for transverse (left) and axial (middle) deformations. (d) Mises stress distribution in the fibers upon a thermal deformation at 40 wt% fiber loading.

Fig. 3 shows the results comparing different nanofiber composites within the same polymer matrix. While NF2 (AR=700) performs better in the FEM simulations than NF1 (AR=40), the experimental results deviate from the simulations much more than the NF1 system. This is likely because the high AR NF2 fibers are more curved or broken during mixing so that the full load-transfer potential of the NF2 system cannot be achieved in reality.

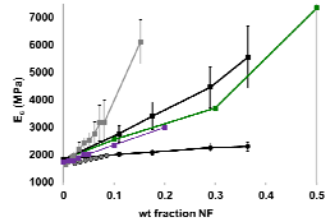

Figure 3: Composite modulus of NF1/polymer (green is experimental data, black is FEM results) and NF2/polymer

systems (purple is experimental data and grey is FEM results) in axial (squares) and transverse (circles) directions.

4.2 Polymer-nanofiber-rubber system

Comparing the FEM simulation results to a model that has been previously verified and to experimental results of a comparable binary system serves to validate the simulation protocol and quantify the errors associated with the assumption of single fiber dispersion. The simulation protocol is now used to predict thermal and mechanical behaviors of more complex systems that cannot be adequately described by simple theories.

Rubbers have been experimentally added to the system to enhance the material's impact properties. However, the low-modulus rubber is expected to lower the overall stiffness and thermal stability of the material. The extent to which the material properties are affected by inclusion of a rubber phase depends on the nanofiber distribution within the polymer and rubber phases. The binary nanofiber/polymer stochastic RVE method described in Sec. 2 has been extended to include a rubber phase where the rubber dispersion diameters are significantly greater than the diameters of nanofibers studied. The large rubber domains pose a challenge to model the nanofibers (diameter ~100 nm) and the rubber (domains ~2 microns) within the same volume element. To resolve this, one quadrant of the rubber particle is modeled as 1/8 of an ellipsoid in the corner of the RVE, as shown in Fig. 4.

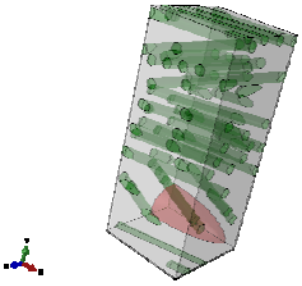

Figure 4**:** 3D representative volume element for the ternary polymer (grey) /nanofiber (green)/rubber (red) composite. Fibers are planarly oriented with a variance of 5 degrees and are excluded from the rubber domain in this example.

The moduli of the ternary nanofiber-rubber-polymer system (FRP) is plotted as a function of fiber loading in the polymer phase in Fig. 5. The fibers have the same statistical distribution as in Fig. 2, but they are excluded from the rubber phase. Since the rubber cannot be adequately described by a linear material model, even at low strains, nonlinear material models described in Sec. 2.2 are used. Fig. 4 compares the modulus computed from nonlinear and linear material model systems. Even for low strain (=.001), the nonlinear models compute a lower composite modulus in both axial and transverse directions for all fiber loadings.

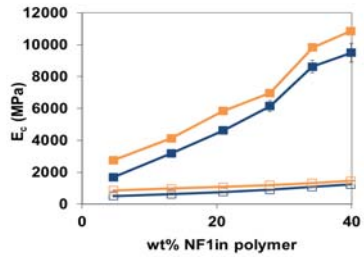

Figure 5: Computed modulus of ternary fiber-rubber-polymer (FRP) system with linear material properties (orange) and nonliinear material properties defined in Sec. 2.2 (blue) in axial (filled squares) and transverse (open squares) directions. Results are for 2D planar fiber orientation with a 5 degree variance about the mean of zero and perfect bonding between all phases.

5 CONCLUSIONS

A new stochastic method to generate RVEs for finite element simulations of nanofiber polymer composites has been developed. The protocol has been validated by comparing the computed tensile modulus and CLTE to experimental values and to the Cox-Krenchel model. The model has been extended to include a rubber phase whose dimensions are 20 times larger than the nanofiber diameters, and realistic material models for all three components. The non-linear constitutive models will allow for accurate simulations even at high strains. At sufficiently high strains, fiber pull-out has been observed experimentally. The FEM algorithm can account for fiber-pull out and imperfect bonding between the rubber and polymer phases phenomenologically by specifying a particular strain at which the bond strength goes from 100% to 0% instantaneously. Results from these parametric studies are ongoing and represent a significant opportunity to gain qualitative understanding on how interfacial interactions affect key mechanical and thermal properties of the ternary nanocomposites.

REFERENCES

[1] J. Bergstrom and J.E. Bischoff, Int. J. Structural Changes in Solids 2, 31, 2010.
[2] J. Bergstrom and M. Boyce, J. Mech. Phys. Solids 46, 931, 1998.
[3] H. L. Cox, British Journal of Applied Physics 3, 72, 1952.
[4] H. Krenchel, *Fiber Reinforcement* (Akademisk Forlag, Copenhagen, 1964).
[5] R. J. Foster, P. J. Hine, and I. M. Ward, Polymer 50, 4018, 2009.
[6] R.A. Schapery, J. Composite Materials 2, 380, 1968.
[7] G. Marom and A. Weinberg, J. Mater. Sci. 10, 1005, 1975.
[8] J.L. Thomason and W.M. Groenewoud, Composites Pt. A 27A, 555, 1996.